APPLIED AND ENVIRONMENTAL MICROBIOLOGY, Aug. 1985, p. 383–391
0099-2240/85/080383-09$02.00/0

Vol. 50, No. 2

Microbial Penetration through Nutrient-Saturated Berea Sandstone

GARY E. JENNEMAN,[1]* MICHAEL J. McINERNEY,[1] AND ROY M. KNAPP[2]

Department of Botany and Microbiology[1] and School of Petroleum and Geological Engineering,[2] University of Oklahoma, Norman, Oklahoma 73019

Received 19 February 1985/Accepted 16 May 1985

Penetration times and penetration rates for a motile *Bacillus* strain growing in nutrient-saturated Berea sandstone cores were determined. The rate of penetration was essentially independent of permeabilities above 100 mdarcys and rapidly declined for permeabilities below 100 mdarcys. It was found that these penetration rates could be grouped into two statistically distinct classes consisting of rates for permeabilities above 100 mdarcys and rates for those below 100 mdarcys. Instantaneous penetration rates were found to be zero order with respect to core length for cores with permeabilities above 100 mdarcys and first order with respect to core length for cores with permeabilities below 100 mdarcys. The maximum observed penetration rate was 0.47 cm · h^{-1}, and the slowest was 0.06 cm · h^{-1}; however, these rates may be underestimates of the true penetration rate, since the observed rates included the time required for growth in the flask as well as the core. The relationship of penetration time to the square of the length of the core suggested that cells penetrated high-permeability cores as a band and low-permeability cores in a diffuse fashion. The motile *Enterobacter aerogenes* strain penetrated Berea sandstone cores three to eight times faster than did the nonmotile *Klebsiella pneumoniae* strain when cores of comparable length and permeability were used. A penetration mechanism based entirely on motility predicted penetration times that were in agreement with the observed penetration times for motile strains. The fact that nonmotile strains penetrated the cores suggested that filamentous or unrestricted growth, or both, may also be important.

In recent years, increased attention has been focused on the microbiology of subterranean aquifers and petroleum reservoirs. This interest was generated by a desire to understand how microorganisms can be used to recover petroleum from reservoirs and how they influence the fate of wastes accidentally or intentionally released into freshwater or saltwater reservoirs (10, 27). The use of microorganisms in the recovery of oil is the main concern of this paper. Microbially enhanced oil recovery (MEOR) is the topic of several recent books and reviews (7, 8, 28). Microorganisms, either indigenous to the subsurface or injected from above ground, are fed a carbohydrate-based medium (e.g., cattle-feed molasses) with the intention of stimulating in situ microbial growth. The in situ growth of microorganisms can be used either to produce cells and associated extracellular polymer for the improvement of reservoir sweep efficiency (18) or to form gases, solvents, or biosurfactants to increase oil mobility in the reservoir (12, 19).

MEOR has stimulated a desire to understand how injected nutrients or chemicals can be metabolized by microorganisms in a porous medium (i.e., rock). It is also of interest to know how water-soluble carbohydrate solutions affect the spread of microbes throughout the porous medium and therefore govern the availability of biological products potentially useful for MEOR. An understanding of the rates at which these processes occur is needed to evaluate the economic and practical feasibility of MEOR. Therefore, it is necessary to understand the kinetics and mechanisms of microbial processes in porous media.

Little information exists on the penetration through rock of microbes under growth conditions. Craw (6) studied the penetration of bacteria out of different filters (Berkefeld, Coulter, etc.) saturated with nutrients and tried to correlate penetration times with the grain size of the filters. However, most work has involved the introduction of dead bacteria or bacteria under non-growth conditions into porous media to study the kinetics of bacterial adsorption and filtration (13, 20). Recent work concerned with plugging rates involving the injection of bacteria under growing conditions was performed in highly permeable rock models (16). However, much residual oil and disposed wastes reside in less permeable rock (e.g., consolidated sandstone). The purpose of this study was to examine the kinetics of microbial growth in relation to microbial penetration times through a consolidated Berea sandstone core. It is shown that relationships exist between penetration time, penetration rate, permeability, and core length. Furthermore, these relationships allow us to speculate about the importance of growth, motility, and chemotaxis in bacterial penetration.

MATERIALS AND METHODS

Bacterial strains. Strain BCI-1NS was isolated from a Berea sandstone core. It is a gram-positive, spore-forming rod occurring both as single cells and in chains. Spores are located subterminally. Individual cells are approximately 4.0 μm long and 0.8 μm wide and are motile.

Strain 140 was isolated from a water sample obtained from the aquifer underlying the Norman municipal landfill. Morphologically, its characteristics are virtually identical to those described for strain BCI-1NS.

Enterobacter aerogenes and *Klebsiella pneumoniae* strains used in this study were obtained from the University of Oklahoma culture collection.

Media and growth conditions. *E. aerogenes* and *K. pneumoniae* strains were each grown in nutrient broth (Difco Laboratories) amended with 1.0% (wt/vol) NaCl and 0.196 (wt/vol) $NaNO_3$. Cultures were grown at 36°C under static conditions.

* Corresponding author.

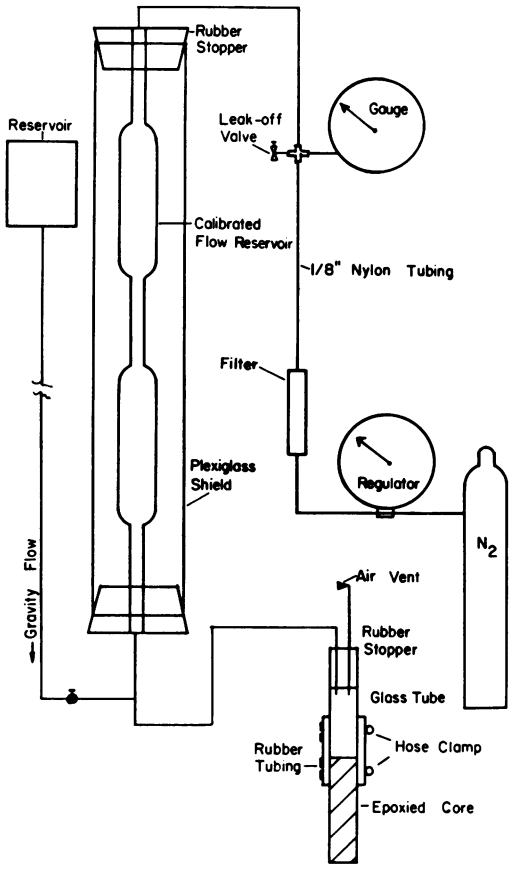

FIG. 1. Permeability apparatus.

Strains BCI-1NS and 140 were each grown in medium E amended with 0.05% (wt/vol) yeast extract (Difco) and 0.1% (wt/vol) $NaNO_3$. Medium E contained (all wt/vol) 5.0% NaCl, 0.1% $(NH_4)_2SO_4$, 0.05% $MgSO_4$, and 1.0% sucrose in 100 mM phosphate buffer (pH 7.0) supplemented with a 1.0% (vol/vol) solution of trace metals (4). Strains BCI-1NS and 140 were grown at 50°C under static conditions and had growth rates of 0.94 and 1.14 h^{-1}, respectively.

Core preparation. Cores were cut from blocks of Berea sandstone (12 by 12 by 6 in) obtained from Cleveland Quarries, Amherst, Ohio. Unless otherwise indicated, the cores were cut into cylinders (diameter, 1.9 cm). Each core was steam cleaned for 2 weeks to remove humic substances and then dried in an oven for 24 h at 125°C. The core was cooled in a desiccator and coated on the sides with Conap Easy-poxy (Fisher Scientific Co.). It was then cut to the desired length.

Growth chambers. Cores used in growth-related experiments were initially autoclaved at 121°C for 30 min while submerged in a 5% (wt/vol) NaCl solution. We found that this step was necessary to purify the epoxy of residual toxic compounds which inhibited the growth of bacteria used in this study (data not shown). After cooling, the core was then placed in a permeability-measuring apparatus (Fig. 1), and the initial permeability (K_0) was determined by using the same brine solution that had been previously filtered through a Millipore filter (pore size, 0.2 μm) to remove small particulate matter.

Each core was then flushed with at least 3 pore volumes (PV) of the respective nutrient medium while still attached to the permeability apparatus. For strains BCI-1NS and 140, medium E with 0.05% (wt/vol) yeast extract and 0.1% (wt/vol) $NaNO_3$ was used. Nutrient broth with 1% (wt/vol) NaCl and 0.1% (wt/vol) $NaNO_3$ was used for the enteric bacteria.

The core was placed in a growth chamber, similar to the one used by Chang and Yen (3), which consisted of two 250-ml Erlenmeyer flasks with a glass nipple (1.9 by 2.5 cm) attached to the bottom of each flask (Fig. 2). The core was then fastened into place with hose clamps and autoclaved for an additional 20 min at 121°C. After cooling, trace metals and $MgSO_4$ were added to 100 ml of medium E in flasks A and B, and the growth chambers were incubated overnight at the respective incubation temperature. Flask A was then inoculated with 1.0% (vol/vol) of the appropriate strain grown in the same medium. The growth chambers were incubated at 50°C for strains BCI-1NS and 140 and at 36°C for the enteric bacteria. Penetration or breakthrough time (t_p) is the time (in hours) elapsed from the time that flask A was inoculated until faintly visible growth appears in flask B. The penetration rate (in centimeters per hour) is the length of the core divided by the penetration time and thus is representative of average rates and not instantaneous rates. Visible growth refers to the point at which faint turbidity appeared in flask B. The cells in flask B were periodically checked by plating on medium E with yeast extract and nitrate to ensure that these cells were of same type as those inoculated into flask A. No growth was observed in uninoculated growth chambers.

Permeability and porosity measurements. Permeability, which is a measure of the fluid conductivity of a porous material, was calculated from Darcy's law:

$$K = \frac{q\mu}{A(\Delta P/L)} \quad (1)$$

where q is the volumetric flow rate (in cubic centimeters per second), μ is the dynamic viscosity of the fluid in centipoise, A is the cross-sectional area of the core (in square centimeters), L is the length of the core (in centimeters), and ΔP is the differential pressure across the core (in atmospheres). The permeability (K) is given in darcys.

The permeability apparatus (Fig. 1) maintains a constant pressure differential across the core. Thus, by measuring the flow rate, the permeability of the core can be calculated. Each core was injected under pressure with a 5% (wt/vol) NaCl brine solution (prefiltered through a Millipore filter [pore size, 0.22 μm]), and the time for a fixed volume of brine to exit the core was measured. The viscosity of the 5%

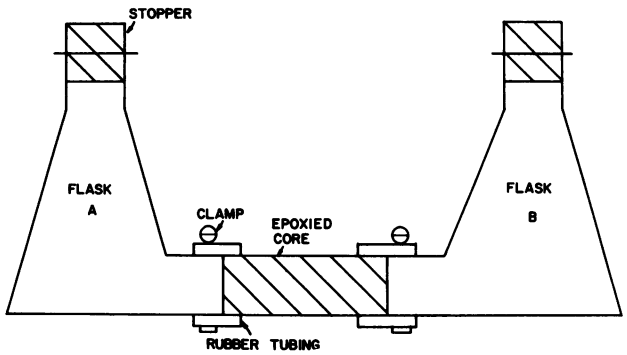

FIG. 2. Growth chamber (modified from that of Jang et al. [17]).

NaCl solution was determined to be 0.91 cP at 38°C. The K_0 was determined after the permeability of the core had stabilized (i.e., permeability values of three successive readings within 5% of each other). At times it was found that flow rate would continuously decrease with increasing volume of brine flushed through the core. When this occurred, the core was backflushed with several PV of brine. After the backflushing, the core was flushed in the original direction of fluid flow and the permeability was calculated from data obtained with the first or second PV of fluid flushed through the core. In most cases, it was found that permeability increased after backflushing, which indicated that the reductions in permeability were probably due to fine migration (11, 21). The Reynolds number for all cores used in these experiments was below 10^{-2}; therefore, permeability measurements were in the region of viscous flow and Darcy's law is valid (5). Initial permeability values also indicated that the epoxy coating provided a good seal between the outside wall of the core and the epoxy, since permeabilities measured were in close approximation to permeability values quoted by Cleveland Quarries. This is very important, since it is desirable to not have bacteria growing between the rock and the epoxy coating.

Porosity was measured by first saturating the core overnight with 5% (wt/vol) NaCl solution under a vacuum. The core was weighed (bulk volume) and then dried in a microwave oven (700 W; Amana) for 12 min at full power and allowed to cool in a desiccator. The core was then weighed again to determine the dry weight. The weight of the brine-saturated core minus the weight of the dry core gave the weight of a pore volume of fluid. The porosity (ϕ) was calculated as

$$\frac{W_{PV}/\rho_B}{\text{Bulk volume}} = \phi \quad (2)$$

where W_{PV} is the weight of a PV of fluid, ρ_B is the density of the 5% NaCl solution (1.02 g/ml), and the bulk volume can be calculated from core dimensions (length × cross-sectional area). The PV was calculated by using the following equation:

$$W_{PV}/\rho_B = \text{PV} \quad (3)$$

Regression analysis. A multiple regression model was developed to establish whether the penetration rates obtained from cores with permeabilities above 100 mdarcys (n = 24) were significantly different from the rates obtained in cores with permeabilities below 100 mdarcys (n = 14):

$$y = B_0 + B^{I}x \quad (4)$$

$$y = B_0 + B^{II}x \quad (5)$$

where y is the penetration rate (in centimeters per hour), x is the independent variable, length (in centimeters), B_0 is the y intercept, and B^{I} and B^{II} are the regression coefficients for rates in cores with permeabilities above and below 100 mdarcys, respectively. The y intercepts were assumed to be equal. The actual values obtained for the y intercept in each case were very close. The hypothesis to be tested was whether the slopes in equations 4 and 5 are equal (H_0: $B^{I} = B^{II}$). The hypothesis was tested by combining equations 4 and 5 and establishing a dummy variable to explain the difference in the slopes ($B^{II} - B^{I}$). If this difference was significantly different from B^{II} or B^{I}, then the null hypothesis was rejected and B^{I} and B^{II} were assumed to be from different populations. The significance test was performed by using a two-tailed t test. The regression routine used also provided information to determine whether B_0, B^{I}, and B^{II} were significantly different from zero. Also, an overall fit of the data to the dependent variable rate, regressed against both length and permeability class, was given by an F test. The R^2 value represented the amount of variance that the overall model explained in terms of the two independent variables. The total analysis was performed by using the REG routine of the Statistical Analysis Systems program (24).

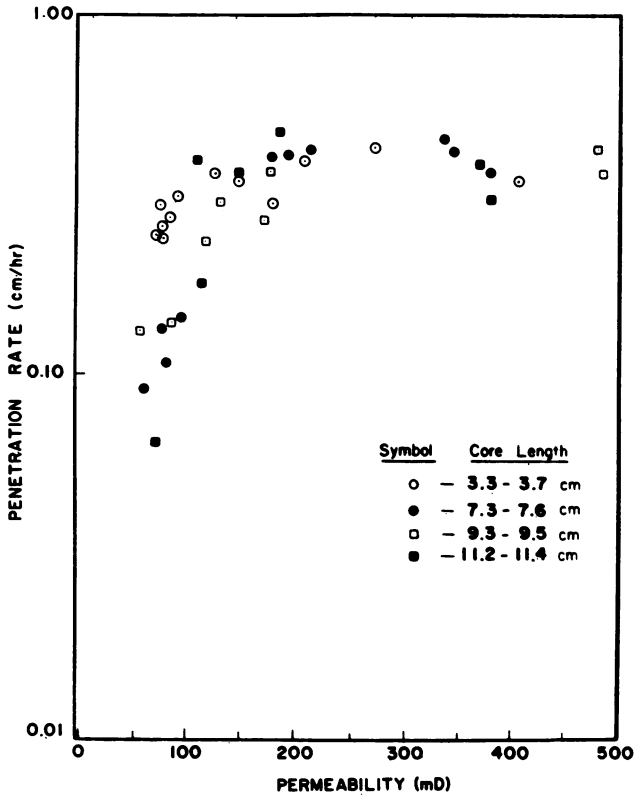

FIG. 3. Effect of permeability on rate of bacterial penetration by strain BCI-1NS. Rates were calculated by dividing penetration times in Fig. 5 by the length of core used.

RESULTS

Effect of length and permeability on penetration. The effect of rock permeability on the rate of microbial penetration of strain BCI-1NS is shown in Fig. 3. Rates were determined for the same bacterium by using Berea sandstone rock cores of varying lengths. The lengths of the cores sampled were evenly distributed within the range of permeabilities tested. The results showed that the rate of penetration was fastest and relatively independent of permeability above 100 to 200 mdarcys and decreased rapidly for cores with permeabilities below this value. The maximum penetration rate measured was 0.47 cm · h^{-1} in an 11.4-cm-long core with a K_0 of 182 mdarcys; the slowest rate measured was 0.06 cm · h^{-1} in an 11.3-cm-long core with a K_0 of 70.7 mdarcys. The lowest permeability examined in this study was approximately 55.0 mdarcys, and the highest was 520 mdarcys. At least two other cores of permeabilities of less than 100 mdarcys with lengths of 11.4 cm were tried, but no growth was observed in flask B for these cores within a 2-week period.

Penetration rates were divided into two classes based on the permeability of the cores. One class was associated with

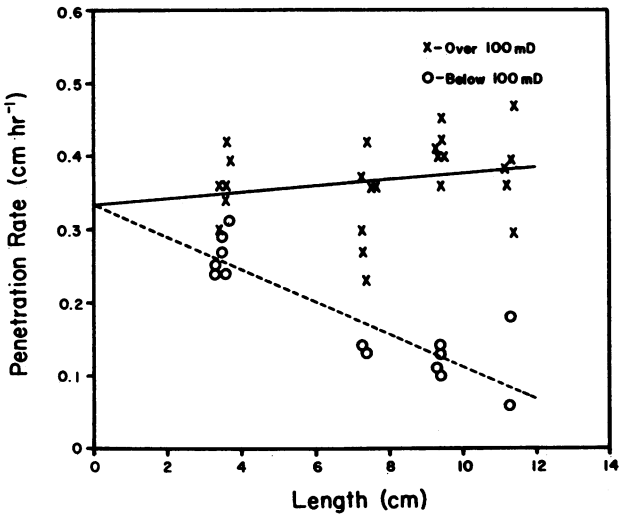

FIG. 4. Effect of core length on rates of bacterial penetration represented in Fig. 3 for strain BCI-1NS growing in medium E amended with 0.05% (wt/vol) yeast extract and 0.1% (wt/vol) sodium nitrate. The solid line represents a least squares, best fit line for cores with permeabilities above 100 mdarcys (×), and the dashed line represents a best fit line for cores with permeabilities below 100 mdarcys (○). These points were replotted from Fig. 3.

cores with permeabilities greater than 100 mdarcys, and another was associated with cores with permeabilities below 100 mdarcys. When these two classes of penetration rates were plotted as a function of the core length, two linear relationships were found (Fig. 4). An overall fit of the entire data set to the multiple regression model described above resulted in a highly significant F value of 0.0001 (Table 1). This indicates that the model accounts very well for the behavior of the dependent variable. Furthermore, an R^2 value of 0.8032 for the overall model was obtained. Thus, approximately 80% of the observed variance in the penetration rates can be explained by the independent variables, core length and permeability class. The remainder of the variance may be explained as experimental error or some other independent variable of the core that was not measured. More importantly, the model indicates that the difference between the slopes ($B^{II} - B^{I}$) is significantly different from zero, which implies that the penetration rates can be grouped into two distinct classes based on permeabilities above and below 100 mdarcys. In the model chosen, the y intercepts for both permeability classes were assumed to be equal, since at a length equal to zero the penetration rate should be independent of the core used when the same bacterium and nutritional conditions were used in all experiments.

If penetration time is plotted as a function of core length for cores with permeabilities above 100 mdarcys, a linear relationship is obtained (Fig. 5A). The slope of the line is equal to 2.5 cm · h^{-1}, and the y intercept is equal to 2.0 h. Therefore, an equation that describes the penetration of strain BCI-1NS through Berea sandstone with permeability above 100 mdarcys is

$$t_p = 2.5L + 2.0 \quad (6)$$

where t_p is the penetration time (in hours) and L is the length of the rock core (in centimeters). The average rate of penetration of strain BCI-1NS calculated from the reciprocal of the slope of equation 6 was 0.4 cm · h^{-1}.

On the other hand, a plot of penetration time against core length for sandstone with permeability below 100 mdarcys yields a curvilinear relationship (Fig. 5B). A fit of the data to a power curve of the general form $y = ax^b$ yields an R^2 value of 0.938. An equation for the curve in Fig. 5B is

$$L = 0.8318\ t_p^{0.5531} \quad (7)$$

where L is the core length (in centimeters) and t_p is penetration time (in hours). If equation 7 is solved as a function of L, the following equation is obtained:

$$t_p = 1.395L^{1.808} \quad (8)$$

which implies that t_p increases in a nearly linear fashion if plotted as a function of L^2 (Fig. 6A). The possible significance of this is explained below.

Importance of cell motility, diffusion, and growth. The effect of cell motility on the penetration time was investigated by using both a motile and a nonmotile enteric bacterium (Table 2). Two taxonomically similar organisms, one (*E. aerogenes*) motile and the other (*K. pneumoniae*) nonmotile, were selected for this experiment. The growth rate of these two organisms under nitrate-respiring conditions (O_2 limited) was 1.38 and 1.11 h^{-1} for *E. aerogenes* and *K. pneumoniae*, respectively. The motile strain penetrated the rock at a rate three to eight times faster than did the nonmotile strain (Table 2). Permeability was not a factor, since penetration time for the nonmotile strain in the highest-permeability core was still approximately four times longer than the longest penetration time for the motile strain.

To examine the role of diffusion or random movement, penetration times were plotted against length. If a core is assumed to be composed of a bundle of capillaries, the movement of cells through a pore should approximate the behavior of cells when moving through a single capillary. Adler and Dahl (1) demonstrated that cell behavior could be described by an equation for diffusion of a thin layer in a column of liquid, for which a plot of time versus the square of the distance that the fastest cells have moved from the origin (L^2) gives a straight line with a y intercept of zero. Our assay is similar to the frontier assay used by Adler and Dahl (1), in which the penetration time is a function of the time for the fastest cells to penetrate some known distance of rock.

TABLE 1. Statistical parameters for multiple regression analysis of rate versus length data[a]

Variable	Statistical parameter		
	Degrees of freedom	Probability > F	Probability > | T |
Overall model	37	0.0001	NA
B_0	1	NA[b]	0.0001
B^{I}	1	NA	0.1149
B^{II}	1	NA	0.0001
$B^{II} - B^{I}$	1	NA	0.0001

[a] The overall model tested is a multiple regression model with the dependent variable rate regressed against two independent variables representing permeability above and below 100 mdarcys. B^{I} and B^{II} are the regression coefficients representing these independent variables, and B_0 is the y intercept, which was assumed to be the same for both permeability classes. The probability > F for the overall model tests how well this model accounts for the behavior of the dependent variables (penetration rate) after adjusting for mean. The probability > | T | represents the significance of B_0, B^{I}, and B^{II} from zero as well as the significance of whether B^{I} is equal to $B^{II}(B^{II} - B^{I})$, from a two-tailed t test. See Fig. 6 for a plot of data; additional explanation is given in the text.

[b] NA, Not applicable.

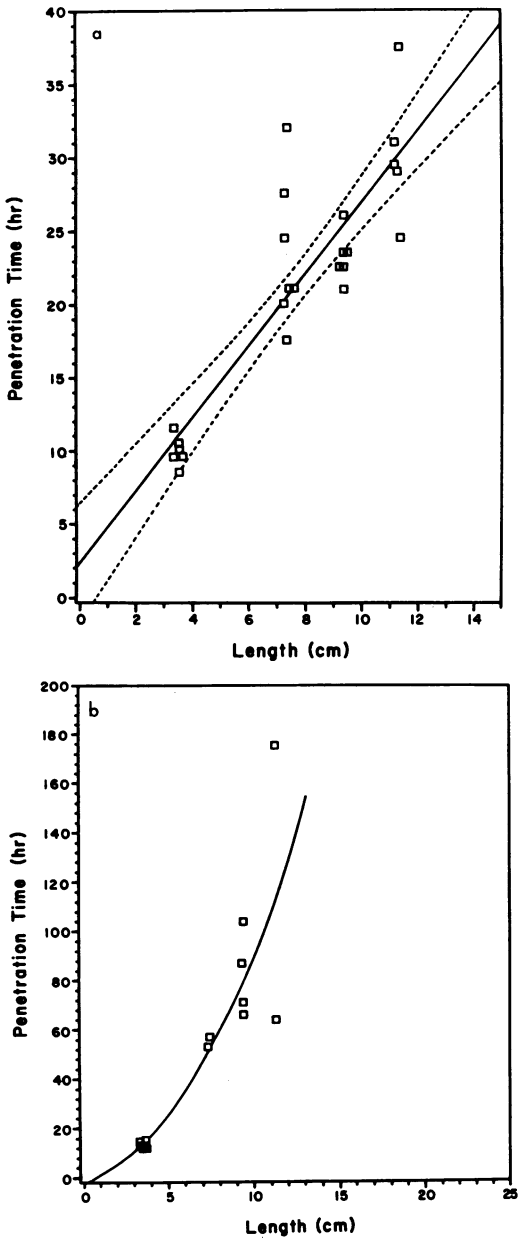

FIG. 5. (A) Effect of core length on penetration time in cores with permeabilities above 100 mdarcys for strain BCI-1NS grown in medium E amended with 0.05% (wt/vol) yeast extract and 0.1% (wt/vol) sodium nitrate. A least-squares linear regression routine was used to plot the line, and its 95% confidence intervals are represented by the dashed lines. A log-anova (Scheffe-Box) test for homogeneity of variances was run on the data and found not to be significant at $P < 0.05$; therefore, the variances were considered homogeneous. (B) Effect of core length on penetration time in cores with permeabilities below 100 mdarcys for strain BCI-1NS grown in medium E amended with 0.05% (wt/vol) yeast extract and 0.1% (wt/vol) sodium nitrate. The curve was fit to the data by using a curve fitting routine designed for an HP-41C (14). The curve is of the general form $y = ax^b$ with a coefficient of determination (R^2) of 0.938, where $a = 1.395$ and $b = 1.808$. A log-anova test of the log-transformed y variable indicated that the transformed variances were not heterogeneous at a significance level of $P < 0.05$. Also, a linear least-squares fit of the transformed data yields an R^2 value of 0.92 indicative that a curvilinear relationship for t_p versus L is valid.

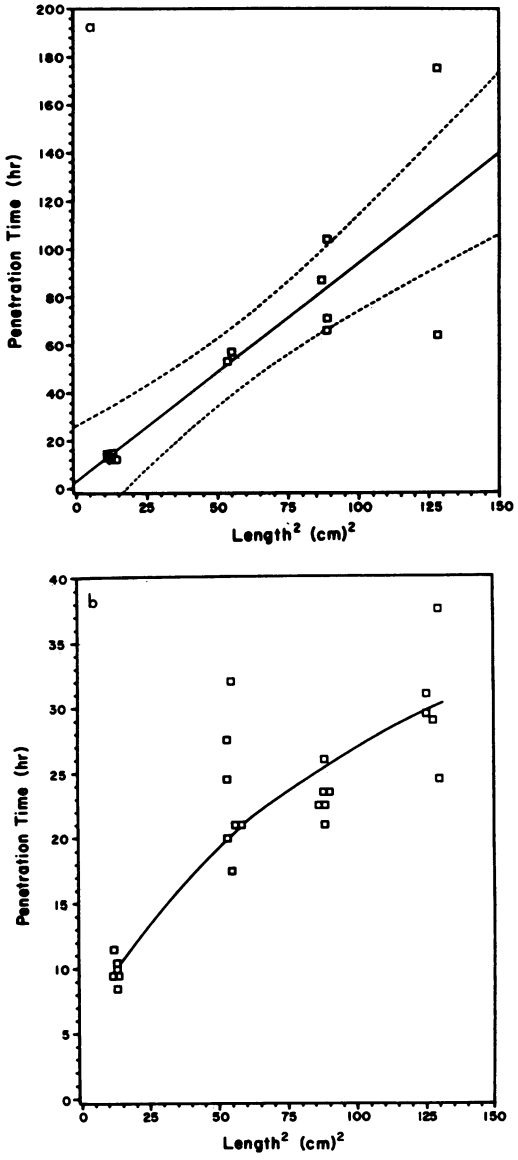

FIG. 6. Relationship between the penetration time and the square of the core length. (A) Cores with permeabilities below 100 mdarcys. The solid line is a least-squares fit of the data, with the dashed lines representing the 95% confidence intervals. Data were replotted from Fig. 5B. Although the data display severe heteroscedasticity of variance, a log transformation of the y variable eliminates this heterogeneity to a nonsignificant level ($P < 0.05$). The rationale for selecting a linear least-squares fit for these data is derived from the fact that equation 8 implies that the relationship of the penetration time and the square of the length should be fairly linear and should pass through the origin.(B) Cores with permeabilities above 100 mdarcys. The data were fit to a power curve of the general form $y = ax^b$ by using a curve fitting routine (14). This equation had the best fit ($R^2 = 0.86$ when $a = 3.152$ and $b = 0.466$) out of the four equations tested, linear ($R^2 = 0.71$), logarithmic ($R^2 = 0.78$), exponential ($R^2 = 0.71$) and power. Data were replotted from Fig. 5A.

In Fig. 6B, for cores with permeabilities above 100 mdarcys, the relationship between t_p and L^2 is curvilinear and therefore does not resemble a diffusion process. However, for cores with permeabilities below 100 mdarcys (Fig. 6A), the relationship is linear with a y intercept near zero, and

TABLE 2. Penetration times of *E. aerogenes* (motile) and *K. pneumoniae* (nonmotile) through Berea sandstone cores

Organism[a]	Core no.	Growth rate (h^{-1})	K_0 (mdarcys)	Length (cm)	Penetration time (h)[b]
E. aerogenes	150		518	4.8	9.5
	151	1.38	611	4.8	9.5
	152		628	4.9	13.5
K. pneumoniae	153		565	4.8	40
	154	1.11	611	4.8	48–55
	155		466	5.0	83

[a] The motility of each strain was checked by inoculating MIO broth (Difco).
[b] Penetration time was the time from inoculation in flask A until visible growth occurred in flask B.

therefore the penetration of cells at least qualitatively resembles diffusion.

The relationship between penetration time and pore volume of the core for both permeability classes is shown in Fig. 7. In both cases, the penetration time is dependent on the pore volume. For cores with permeabilities greater than 100 mdarcys, the penetration time increased linearly with pore volume, whereas penetration time increased exponentially with pore volume for cores with permeabilities below 100 mdarcys. These data exclude the possibility that growth occurs inside the core as it does outside the core, i.e., that the time required to observe visible growth is dependent only on the liquid volume. If growth is not restricted by the presence of the core and penetration time is a function only of total liquid volume, one would predict that the observed penetration times would be independent of the pore volume of the cores (usually less than 1 ml), since this volume is only a small fraction of the volume in flask B (100 ml) (Fig. 7, dashed line). The experimental data show that penetration time is not independent of pore volume, and thus growth inside the core does not occur in an unrestricted sense as it would in a flask.

On the other hand, if growth is perceived to occur in a filamentous fashion through the core, t_p would be described as follows:

$$t_p = t_d \left[\frac{\ln (l_x/l_c)}{\ln 2} \right] \tag{9}$$

where t_p is the penetration time (in hours), l_x is the length of the core penetrated, l_c is the length of the bacterial cell (calculated as 4.0×10^{-6}m), and t_d is the doubling time (in hours) of strain BCI-1NS ($t_d = 0.74$ h). This, of course, only represents the time for a cell to traverse the length of the core and not the additional time required to reach faintly visible turbidity. An equation that represents the entire process would be:

$$t_p = t_d \left[\frac{\ln (l_x/l_c)}{\ln 2} \right] + \frac{\ln X_t - \ln X_0}{\mu} \tag{10}$$

where X_t is the number of cells at some time t, X_0 is the number of cells at time zero, and m is the specific growth rate (in reciprocal hours). The second term represents the additional time required for a single cell entering flask B to reach faintly visible turbidity (estimated at 10^6 cells · ml^{-1}). Therefore, assuming that a single cell entered the core at time t, we predict that strain BCI-1NS would take 9.7 h + 19.6 h, or 29.3 h, to reach faintly visible turbidity if penetrating a core of a length of 3.5×10^{-2} m. This represents the fastest penetration time possible for this model, since we are assuming the cell takes a straight path through the core. However, the observed penetration time for a core of this length was approximately 12 h (at least 2.5 times faster).

If motility is assumed to be the mechanism for microbial penetration, then the observed results should be predicted by the following equation:

$$t_p = l_x/v_m + (\ln X_t - \ln X_0)/\mu \tag{11}$$

where v_m is the actual velocity of the motile cell (in centimeters per hour) and l_x is the length (in centimeters) of the path from flask A to flask B (i.e., core length), and again the second term explains the time for a single cell in flask B to reach faintly visible turbidity. If an actual velocity of 10 cm · h^{-1} (actual velocity of *Escherichia coli* as measured by Adler and Dahl [1]) is assumed for strain BCI-1NS, it is predicted that a single cell would take 0.35 h + 19.6 h, or 19,96 h, to reach faintly visible turbidity in flask B; however, the observed time is almost twice as fast.

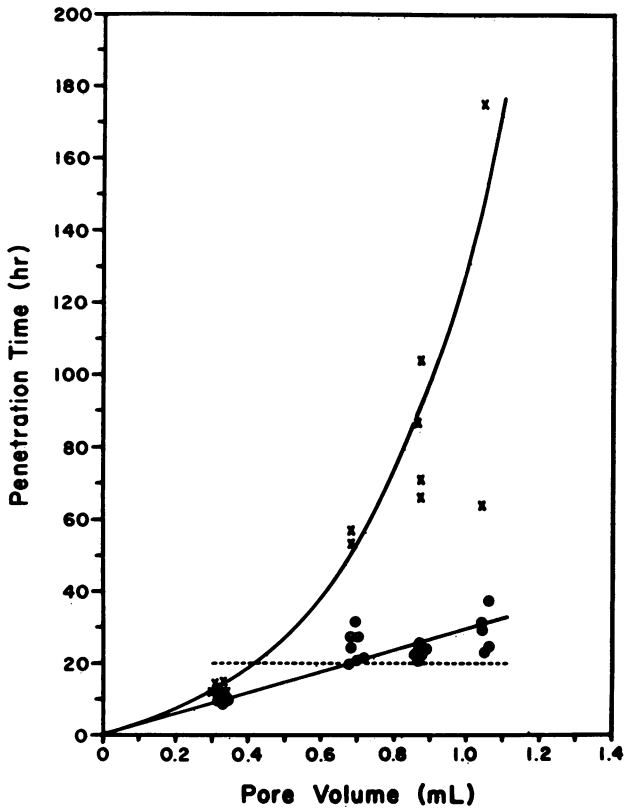

FIG. 7. Relationship between pore volume of the core and penetration time for cores with permeabilities below (×) and above (○) 100 mdarcys. The dashed line represents the theoretical relationship when penetration through the core is assumed to occur as unrestricted growth. The theoretical relationship was calculated by using the equation

$$t_p = (\ln X_t - \ln X_0)/\mu,$$

where X_t is the number of cells needed to give faint turbidity in flask B (estimated at 10^8 cells per 100 ml) plus the number of cells contained in 1 PV of the core (estimated to be insignificant compared with the number of cells in flask B), X_0 is the number of cells entering the core from flask A (assumed to be 1), and μ is the specific growth rate of strain BCI-1NS (0.94 h^{-1}) experimentally determined in a flask containing medium E with $NaNO_3$ and yeast extract.

In another experiment, a washed-cell preparation of strainBCI-1NS was suspended in a 5% NaCl–100 mM phosphate buffer contained in flask A. The cell suspension in flask A had a final concentration of 10^7 cells · ml^{-1}, and penetration of these cells through a cylindrical Berea core (3.5 by 0.75 cm; permeability, 200 mdarcys) into flask B was monitored for a 24-h period by plating 0.1 ml on medium E containing yeast extract and nitrate. No cells were detected in core B within the period tested. This was twice the time required for penetration to occur if nutrients were present; however, it is possible that fewer than 10 cells · ml^{-1} penetrated the core within the period checked, since this is below the detection limits of the plating method used.

DISCUSSION

Myers and Samiroden (22), while studying the penetration of ^{32}P-labeled *Serratia marsecens* cells in oil-containing sandstone and limestone cores of differing permeability and porosity, found no relationship between the rate of penetration and either the permeability or the porosity of the rock. However, our results indicate that in nutrient-containing, brine-saturated Berea sandstone the rate of bacterial penetration in cores above approximately 100 mdarcys is essentially independent of permeability, whereas below 100 mdarcys the rate decreases rapidly with decreasing permeability. Conditions favoring inbibition of cells and brine were used by Myers and Samiroden (22) as a means of cell penetration, whereas our results were achieved under static conditions favoring growth, chemotaxis, and motility. Therefore, it would appear that if bacterial cells are allowed to penetrate rock by their own locomotion, their rate of penetration can be predicted on the basis of the rock permeability. Craw (6), while investigating the penetration of bacteria out of nutrient-saturated Doulton, Pasteur, Berkefeld, and Slack and Brownlow filters, concluded that the grain size of the filter mass was the most important factor governing the growth of bacteria through the filters. For a relatively homogeneous rock like Berea sandstone, it is plausible to assume that with decreasing permeability or grain size of rock, the median pore throat size of the rock decreases with decreasing permeability; however, in many instances the rock is highly stratified with respect to permeability and this assumption would not necessarily be the case. Therefore, it is probable that one of the major factors controlling the rate of penetration is pore throat size. Updegraff and Wren (25, 26) found that the pore throat size of the rock should be at least twice the cell size to allow passage of cocci or bacilli through rock when cells suspended in brine were pumped into the rock. Kalish et al. (20), using Berea sandstone of different permeability ranges (278 to 400 mdarcys, high; 130 to 162 mdarcys, medium; and 17.7 to 48.3 mdarcys, low), found that the median pore size distribution of the cores was 3.5 to 4.0 μm for the low-permeability range, 4.5 to 5.0 μm for the medium-permeability range, and 5.5 to 6.0 μm for the high-permeability range. Nazarenko et al. (23), as well as Zvyagintsev and Pityruk (29), while studying the growth of bacteria and yeast in small capillaries of rectangular cross-section, found that growth rates and cell sizes decreased and lag times increased with decreasing rectangular cross-section. In fact, in rectangular cross-sections with dimensions of 8 by 4 μm, no increase in cell number was observed for *Bacillus subtilis* strains when growing under nutrient-rich conditions. Therefore, it seems that pore throat size and permeability should influence bacterial penetration in sandstone.

Mechanisms for penetration of motile cells could include growth, motility, chemotaxis, or maybe even a combination of these modes of locomotion. Our results suggest that the mode of penetration must be some function of the length of the core. Therefore, an unrestricted growth model as described in Fig. 7 cannot entirely explain our results, since the penetration time for this model is essentially independent of length and pore volume for the length of rock core examined. The penetration times for the filamentous growth model are a function of the length of the core; however, it is conceptually difficult to visualize a chain of cells elongating at an exponential rate along a tortuous path. Furthermore, this model predicts that penetration times should be 2.5 times longer than those we observed. Therefore, the theoretical model which best explains the observed penetration times is one based on motility. As mentioned above, equation 11 predicts that a cell takes approximately 20 h to travel 3.5 cm if we assume that equation 11 is valid. This value is still almost twice as long as the observed penetration time of 9 to 12 h. However, shorter penetration times are predicted by equation 11 if more than a single cell simultaneously enter flask B or at least enter within the time required for one doubling of the cell population. Jang et al. (17) recorded a penetration time of 24 h for a *B. subtilis* isolate to penetrate 3.81 cm of Berea rock with a permeability of approximately 400 mdarcys; they used the time to reach visible turbidity in the outlet flask as part of the total penetration time. Chang and Yen (3) found that only 45 min was required in a similar growth chamber for about 10^2 cells of *Escherichia coli* B per ml to be present in flask B after penetrating a 2.5-cm length of Berea sandstone (permeability, 400 mdarcys). Our results for penetration time versus the square of the length for high-permeability cores (Fig. 6) are consistent with the kind of movement that Adler and Dahl described as band-like, which means that the cells move as a front such that more than one cell could reach flask B simultaneously. However, Adler and Dahl (1) were working with auxotrophic mutants capable of chemotaxis and motility but not capable of growth in the test medium. If we assume that 10^1 to 10^2 cells · ml^{-1} entered flask B within the time for one doubling to occur, as found by Chang and Yen (3), equation 11 predicts penetration times of 10 to 12.5 h, which are well within our observed times. However, for longer core lengths, equation 11 predicts that shorter penetration times would occur than those we observed; these longer penetration times are possibly due to fewer and fewer cells entering flask B simultaneously as a result of an increasing number of pore throat constrictions that restrict cell passage at longer core lengths.

In low-permeability cores, penetration times increased exponentially with length, whereas in high-permeability cores a linear relationship with length was found. This does not preclude the possibility that at shorter core lengths, cells in both high- and low-permeability cores could not have penetrated the entire length in similar periods. This would be possible if it is assumed that fewer cells reach flask B simultaneously in low-permeability cores, which would increase the time required to reach faintly visible turbidity. This possibility is further substantiated by the fact that penetration of cells through these low-permeability cores at least qualitatively resembles diffusion. Adler and Dahl (1) demonstrated that cells that exhibited a diffusion-like penetration in glass capillaries were nonchemotatic cells that moved randomly and not as a uniform band of cells. Since in our experiments no attempt was made to eliminate chemotaxis, the diffusion-like movement in low-permeability cores is most probably due to some property of the rock. If it is

assumed that rock is made up of a network of capillaries and that in general as permeability decreases the pore diameter of these capillaries decreases, then it is evident that as permeability decreases and length increases the probability becomes greater that a larger number of these capillaries reach some constriction inaccessible to bacterial penetration. Therefore, the fact that penetration time in low-permeability cores is directly proportional to the square of the length could imply that the actual path taken by the bacterium is longer than the sample path. This phenomenon is often described in petrophysical terms as tortuosity.

If motility is indeed the major mode of penetration for cells through rock, the problem of how non motile cells penetrate rock is a puzzling one. Our results (Table 2) indicated that nonmotile cells do penetrate Berea sandstone, although at a slower rate than motile cells. This slower rate could be explained by the filamentous growth model. However, as previously mentioned, it is conceptually difficult to envision a filament of cells expanding exponentially along a tortuous path. It is more likely that a mode of penetration consisting of both filamentous and nonfilamentous (i.e., unrestricted) growth would occur. It is not likely that diffusion, convection, and Brownian movement play a significant role in movement because of the large size of the bacterial cells. Hirsch and Christensen (15) found that filamentous growth, such as occurs with actinomycetes, enables these organisms to penetrate Millipore membrane filters of pore size 0.22 μm, whereas nonfilamentous bacteria could not penetrate the same filters. Also, it is possible that the cells generate enough gas inside the rock pores that localized pressure increases may act to push these nonmotile cells through larger pores. Experiments involving the use of nonmotile cells penetrating various lengths of rock could help to further elucidate the mechanism.

Information regarding the instantaneous rate of bacterial penetration would also be very helpful in increasing our understanding of bacterial penetration of porous rock. We have already mentioned penetration rate and its relationship to permeability; however, these rates are representative of average rates and not instantaneous rates. For a measurement of instantaneous rates, the experiments measuring penetration time against length would have to be done on the same rock sample. Such measurements would be very difficult if not impossible to perform on intact pieces of consolidated rock. If we can assume that the cells behave similarly in a whole piece of rock as they would if the whole were divided into separate lengths, we could derive an apparent rate equation from Fig. 5 for cores with permeabilities above and below 100 mdarcys. This assumption may not be unreasonable, since tests were performed on a relatively homogenous rock such as Berea sandstone. Therefore, a rate equation for penetration in cores with permeabilities above 100 mdarcys is the derivative of equation 6 with respect to t_p:

$$dt_p = 2.5\, dL \tag{12}$$

$$dL/dt_p = 0.4 \tag{13}$$

where t_p is penetration time and L is core length. Equation 13 represents a zero-order rate expression, and thus the penetration rate would be independent of length at permeabilities greater than 100 mdarcies. This implies that neither pore size nor tortuosity is restrictive to bacterial penetration in high-permeability cores. For low-permeabilty cores the apparent rate equation is the derivative of equation 8 with respect to t_p:

$$dt_p = 2.522L^{0.808}dL \tag{14}$$

$$\mathrm{d}L/dt_p = 0.396L^{-0.808} \tag{15}$$

This rate expression is very close to a first-order rate equation and further indicates that penetration rate decreases with increasing core length. This supports our conclusion that in low-permeability cores, decreasing pore throat sizes result in the presence of a greater number of constrictions that are restrictive to bacterial penetration. The number of these constrictions increases with increasing length of rock core, meaning that the cell must travel a path which could be much longer than the sample path. Also, fewer and fewer cells are found per area of rock as length increases, since many cells are retained in constrictions at the proximinal end of the core with respect to inoculation. There is also an increasing probability with decreasing pore size that many cells do not even enter the core because fewer pores are accessible. Therefore, the apparent decrease in penetration rate with core length may not actually reflect the slowing down of the cells as they penetrate longer core lengths, but may simply indicate that fewer and fewer cells are found per unit area as cells penetrate further into the rock. Thus, only a few cells, if any, reach flask B at any given moment, which results in an increased time until faintly visible growth occurs in flask B than if the cells were arriving as a front or band.

As far as MEOR is concerned, these results have interesting implications for processes which rely on the ability of microorganisms to preferentially grow and plug high-permeability regions of a reservoir (i.e., selective plugging) while, it is hoped, not plugging the low-permeability zones, which have higher oil saturations. According to our results, penetration should occur to the greatest extent in these higher-permeability regions and cause the greatest permeability reduction in these areas, whereas plugging in the low-permeability zones (higher oil saturation) should be more superficial and occur more slowly. It has often been stated (9, 25, 26) that ca. 100 mdarcys is the lowest permeability at which effective cell penetration can occur, and our results further substantiate this claim. However, it should be remembered that permeability is not always a good indicator of pore throat size, and thus 100 mdarcys may not be limiting for all types of rocks or reservoirs. Instead, it would probably be more correct to correlate bacterial penetration with pore throat size and tortuosity, which is a measure of the interconnectedness of flow paths along the length of a core. Other types of sandstone along with limestone must be tested to determine whether similar relationships of penetration with permeability and length exist. We can conclude from our results that cells that are best suited for MEOR processes should be motile; however, it is hoped that future work with chemotatic and motility mutants (2) can further elucidate the mechanism of bacterial penetration for both motile and nonmotile cells.

ACKNOWLEDGMENTS

This work was supported under contract no. DE-AC19-80BC10300 from the U.S. Department of Energy as well as a grant from the Energy Resources Institute at the University of Oklahoma, Norman.

We thank A. Schwarzkopf and J. Winters for their assistance with multiple regression analysis. We also acknowledge the helpful comments made by D. E. Menzie and J. Suflita as well as the help of R. Raiders for core preparation and J. Power for assistance with illustrations. A special thanks to S. Russell for typing and S. Duda and S. Heinrichs for the artwork.

LITERATURE CITED

1. **Adler, J., and M. M. Dahl.** 1967. A method for measuring the motility of bacteria and for comparing random and non-random motility. J. Gen. Microbiol. **46**:161–173.
2. **Armstrong, J. B., J. Adler, and M. M. Dahl.** 1967. Nonchemotactic mutants of *Escherichia coli*. J. Bacteriol. **93**:390–398.
3. **Chang, P. L., and T. F. Yen.** 1984. Interaction of *Escherichia coli* B and B/4 and bacteriophage T4D with Berea sandstone rock in relation to enhanced oil recovery. Appl. Environ. Microbiol. **47**:544–550.
4. **Clark, J. B., D. M. Munnecke, and G. E. Jenneman.** 1981. *In situ* microbial enhancement of oil recovery. Dev. Ind. Microbiol. **22**:695–701.
5. **Collins, R. E.** 1976. Flow of fluids through porous materials, p. 52. The Petroleum Publishing Co., Tulsa, Okla.
6. **Craw, J. A.** 1908. On the grain of filters and the growth of bacteria through them. J. Hyg. **8**:70–73.
7. **Donaldson, E. C., and J. B. Clark (ed.).** 1982. International Conference on Microbial Enhancement of Oil Recovery. Proceedings, U.S. Department of Energy, Bartlesville Energy Technology Center, Bartlesville, Okla. (Available through National Technical Information Service [CONF 8205140].)
8. **Finnerty, W. R., and M. E. Singer.** 1983. Microbial enhancement of oil recovery. Biotechnology **1**:47–54.
9. **Forbes, A. D.** 1980. Micro-organisms in oil recovery, p. 169–180. *In* D. E. F. Harrison, I. J. Higgins, and R. Watkinson (ed.), Hydrocarbons in biotechnology. Heyden and Son, Ltd., London.
10. **Ghiorse, W. C., and D. L. Balkwill.** 1983. Enumeration and morphological characterization of bacteria indigenous to subsurface environments. Dev. Ind. Microbiol. **24**:213–224.
11. **Gruesbeck, C., and R. E. Collins.** 1982. Entrapment and deposition of fine particles in porous media. Soc. Pet. Eng. J. **22**:847–856.
12. **Grula, E. A., H. H. Russell, D. Bryant, M. Kenaga, and M. Hart.** 1982. Isolation and screening of clostridia for possible use in microbially enhanced oil recovery, p. 43–47. International Conference on the Microbial Enhancement of Oil Recovery. *In* E. C. Donaldson and J. B. Clark (ed.), Proceedings, U.S. Department of Energy. Bartlesville Energy Technology Center, Bartlesville, Okla. (Available through National Technical Information Service [CONF 8205140].)
13. **Hart, R. T., T. Fekete, and D. L. Flock.** 1960. The plugging effect of bacteria in sandstone systems. Can. Min. Metall. Bull. **53**:495–501.
14. **Hewlett-Packard Co.** 1981. Standard applications handbook—HP-41C. Hewlett-Packard Co., Corvallis, Oreg.
15. **Hirsch, C. F., and D. L. Christensen.** 1983. Novel method for selective isolation of actinomycetes. Appl. Environ. Microbiol. **46**:925–929.
16. **Jack, T. R., B. G. Thompson, and E. DiBlasio.** 1982. The potential for use of microbes in the production of heavy oil, p. 88–93. International Conference on the Microbial Enhancement of Oil Recovery. *In* E. C. Donaldson and J. B. Clark (ed.), Proceedings, U.S. Department of Energy. Bartlesville Energy Technology Center, Bartlesville, Okla. (Available through National Technical Information Service [CONF 8205140].)
17. **Jang, L.-K., P. W. Chang, J. E. Findley, and T. F. Yen.** 1983. Selection of bacteria with favorable transport properties through porous rock for the application of microbial-enhanced oil recovery. Appl. Environ. Microbiol. **46**:1066–1072.
18. **Jenneman, G. E., R. M. Knapp, M. J. McInerney, D. E. Menzie, and D. E. Revus.** 1984. Experimental studies of *in-situ* microbial enhanced oil recovery. Soc. Pet. Eng. J. **24**:33–37.
19. **Jenneman, G. E., M. J. McInerney, R. M. Knapp, J. B. Clark, J. M. Feero, D. E. Revus, and D. E. Menzie.** 1983. A halotolerant, biosurfactant-producing *Bacillus* species potentially useful for enhanced oil recovery. Dev. Ind. Microbiol. **24**:485–492.
20. **Kalish, P. J., J. E. Stewart, W. F. Rogers, and E. O. Bennett.** 1964. The effect of bacteria on sandstone permeability. J. Pet. Technol. **16**:805–814.
21. **Mungan, N.** 1965. Permeability reduction through changes in pH and salinity. J. Pet. Technol. **17**:1449–1453.
22. **Myers, G. E., and W. D. Samiroden.** 1967. Bacterial penetration in petroliferous rock. Prod. Mon. **31**:22–25.
23. **Nazarenko, A. V., A. I. Nesterov, A. P. Pitryuk, and V. M. Nazarenko.** 1974. Growth of methane-oxidizing bacteria in glass capillaries. Mikrobiologiya **43**:146–151.
24. **Ray, A. A. (ed.).** 1982. SAS user's guide, p. 39–84. SAS Institute Inc., Cary, N.C.
25. **Updegraff, D. M.** 1982. Plugging and penetration of reservoir rock by microorganisms, p. 80–85. International Conference on the Microbial Enhancement of Oil Recovery. *In* E. C. Donaldson and J. B. Clark (ed.), Proceedings, U.S. Department of Energy. Bartlesville Energy Technology Center, Bartlesville, Okla. (Available through National Technical Information Service [CONF 8205140].)
26. **Updegraff, D. M., and G. B. Wren.** 1954. The release of oil from petroleum-bearing materials by sulfate-reducing bacteria. Appl. Microbiol. **2**:309–322.
27. **Wilson, J. T., J. F. McNabb, D. L. Balkwill, and W. C. Ghiorse.** 1983. Biotransformation of selected organic pollutants in ground water. Dev. Ind. Microbiol. **24**:225–233.
28. **Zajic, J. E., D. C. Cooper, T. R. Jack, and N. Kosaric.** 1983. Microbial enhanced oil recovery. Pennwell Publishing Co., Tulsa, Okla.
29. **Zvyagintsev, D. G., and A. P. Pitryuk.** 1973. Growth of microorganisms of various sizes under continuous flow and static conditions. Mikrobiologiya **42**:60–64.